*Biosci. Biotechnol. Biochem.*, **65** (10), 2233–2242, 2001

# Catalytic Function of the Residues of Phenylalanine and Tyrosine Conserved in Squalene-Hopene Cyclases

Tsutomu SATO and Tsutomu HOSHINO†

*Department of Applied Biological Chemistry, Faculty of Agriculture, and Graduate School of Science and Technology, Niigata University, Ikarashi, Niigata 950-2181, Japan*

Received April 9, 2001; Accepted May 18, 2001

**Site-directed mutagenesis experiments on all the conserved residues of Phe and Tyr in all the known squalene-hopene cyclases (SHCs) were carried out to identify the active site residues of thermophilic *Alicyclobacillus acidocaldarius* SHC. The following functions are proposed on the basis of kinetic data and trapping of the prematurely cyclized products: (1) The Y495 residue probably amplifies the D376 acidity, which is assumed to work as a proton donor for initiating the polycyclization cascade, but its role is moderate. (2) Y609 possibly assists the function of F365, which has previously been assigned to exclusively stabilize the C-8 carbocation intermediate through cation-$\pi$ interaction. The Y609A mutant produced a partially cyclized bicyclic triterpene. (3) Y612 works to stabilize both the C10 and C8 carbocations, this being verified by the finding that mono- and bicyclic products were formed with the Y612A mutant. (4) F129 was first identified to play a crucial role in catalysis. (5) The three residues, Y372, Y474 and Y540, are responsible for reinforcing the protein structure against thermal denaturation, Y474 being located inside QW motif 3.**

**Key words:** squalene; hopene; triterpene; terpene cyclase; *Alicyclobacillus acidocaldarius*

The conversion of squalene **1** into pentacyclic hopene **2** and hopanol **3** is one of the most complicated biochemical reactions (Scheme 1).[1–3] This reaction is mediated by squalene-hopene cyclases (SHC) [EC 5.4.99-] which are found in prokaryotic bacterium species. The polycyclization process proceeds under precise enzymatic control to form five new rings and nine new chiral centers (Scheme 1). Very recently, we have demonstrated that two ring-expansion processes were involved during the polycyclization reaction.[4,5,7] The 5-membered C- and D-rings were formed according to Markovnikov closure, and subsequently

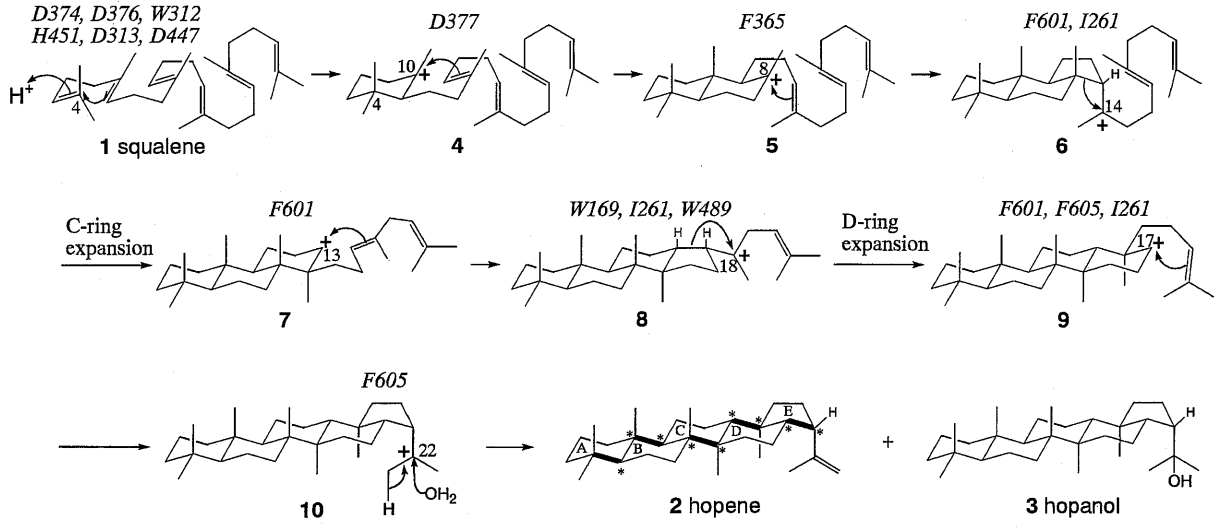


**Scheme 1.** Proposed Cyclization Mechanism for Squalene **1** into Hopene **2** and Hopanol **3** by SHC.
The production ratio of **2** to **3** was ca. 5:1. The polycyclization proceeds with precise enzymatic control to form five new C–C bonds (bold line) and nine new chiral centers ( * ). The active site residues, which are assigned by site-directed mutagenesis,[3–6,11,14–21] are also indicated by italic letters.

† To whom correspondence should be addressed. FAX: +81-25-262-6854; E-mail: hoshitsu@agr.niigata-u.ac.jp
*Abbreviations*: SHC, squalene-hopene cyclase; OSC, oxidosqualene cyclase

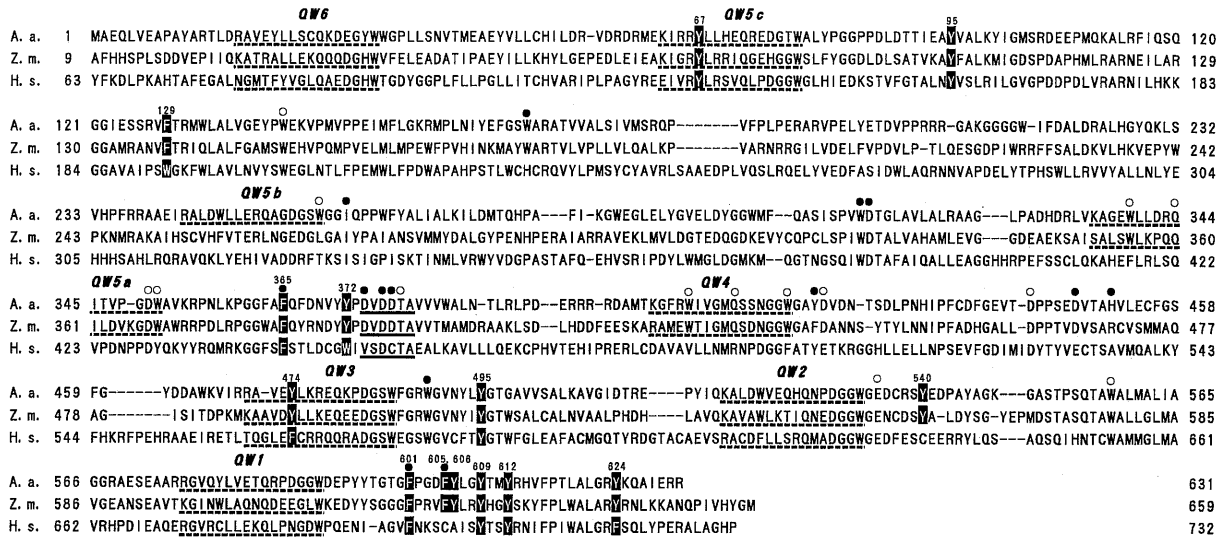


**Fig. 1.** Amino Acid Alignment of *Alicyclobacillus acidocaldarius* SHC (A.a.), *Zymomonas mobilis* SHC (Z.m.) and *Homo sapiens* OSC (H.s.).

The Phe and Tyr residues conserved in all SHCs are shaded. The solid underline shows the DXDDTA or VXDCTA motif. Dotted underlines indicates the QW motifs. The active site residues, which were identified in the previous studies,[3-6,11,14-21] are designated by the symbol ●. The components responsible for protein stabilization[14,15] are marked with ○. The numbering of the QW motifs is according to ref. 14.

undergo ring-expansion reactions into the corresponding 6-membered rings (anti-Markovnikov adducts) of hopane skeleton **2**. The cationic intermediates, **6** and **8**, were trapped by using substrate analogs having a highly nucleophilic hydroxy group, due to the significantly longer lifetime of **6** and **8** during the polycyclization reaction. Anti-Markovnikov intermediate **9** was also trapped by changing the large steric bulk size (Ile) into a smaller one (Ala) at the 261-position; **9** was named prohopane skeleton.[6] We have proposed that the polycyclization reaction proceeds as shown in Scheme 1.[3-6] (3*S*)-2,3-Oxidosqualene also undergoes similar polycyclization reactions by eukaryotic oxidosqualene cyclases (OSC), leading to the construction of a variety of triterpene skeletons such as lanosterol for animals, yeast and fungi, and cycloartenol, lupeol and $\beta$-amyrin for plants.[1,2] Seven SHCs and ca. thirty OSCs have been cloned and sequenced.[8-10] Figure 1 depicts the amino acid alignment of two SHCs from *Alicyclobacillus acidocaldarius* (Gram-positive) and *Zymomonas mobilis* (Gram-negative), and of OSC from *Homo sapiens* as typical examples. A comparison of SHCs with OSCs has shown about 30% of identity with regard to the primary structures and revealed the involvement of specific amino acid sequence repeats, the so-called QW motif, in all the SHCs and OSCs (Fig. 1).[8] The DXDDTA motif conserved in prokaryotic SHCs has also been noted, which corresponds to the VXDCTA motif in eukaryotic OSCs. Overexpression of the cyclase in *Escherichia coli*[11,12] and a three-dimensional X-ray structure[12,13] have been attained for *A. acidocaldarius* SHC. In the past few years, there have been remarkable advances on the identification of active site residues. Site-directed mutagenesis experiments, which have been carried out by us and Poralla's group, have allowed the characterization of the catalytic function of some important amino acids.[3-6,11,14-21] The site-directed mutagenesis experiments on all the conserved Trp and all the acidic residues of Asp and Glu have demonstrated that not all of the QW motifs were active sites,[14] and that the D374XD376D377TA motif served a proton on the terminal double bond of **1** to initiate polycyclization. Carbocation **4** is likely to be stabilized by the carboxylate anion of D377.[15] Cation-$\pi$ interaction is now widely accepted as the main driving force for the cyclization cascade, which has been verified by point mutation experiments on F365, F601 and F605.[5,16,17] It is quite interesting to answer the question of how stereochemical control can be achieved by the cyclase enzyme, leading to the construction of only one isomer **2** despite $2^9$ stereoisomers being possible (nine chiral centers in **1**). We have already demonstrated that the steric bulk size of the amino acid residue controls the stereochemical destiny; the replacement of Ile by less bulky Ala or Gly at the 261-position resulted in the production of compounds having the stereochemistry different from that of the true intermediates.[6] Some amino acids crucial for polycyclization catalysis are illustrated in Scheme 1.

The aromatic residues are unusually abundant among SHCs and OSCs.[8-10] Functional analyses of all conserved Trp residues have been completed by us,[14] but those of the Phe and Tyr residues remain inadequate. In *A. acidocaldarius* SHC, four Phe residues are conserved at positions 129, 365, 601 and 605, and ten Tyr residues at positions 67, 95, 372,

474, 495, 540, 606, 609, 612 and 624 (Fig. 1). Three residues of F365, F601 and F605, out of the 14 residues, have previously been shown to stabilize the transient carbocation intermediates *via* cation-$\pi$ interaction. F365 stabilized the C-8 cation of **5**,[16] F601 facilitated the C-ring expansion of **6**→**7**,[5] and F605 catalyzed the D-ring expansion reaction of **8**→**9** by stabilizing cationic intermediates **9** and **10** (Scheme 1).[17] However, the functions have remained unclear of the remaining 11 residues of Phe and Tyr. To characterize the role of the $\pi$-electron in the aromatic ring, these 11 aromatic residues were mutated into aliphatic Ala in the present study. Very recently, functional analyses of Y495, Y609 and Y612 have been reported by mutating Tyr into Phe to examine the effect of the phenolic hydroxyl group on polycyclization.[21] However, these functional analyses were not sufficient, because the Phe mutants had still aromatic $\pi$-electrons, and no kinetic values such as $K_m$ and $k_{cat}$ have been reported by using homogeneously purified SHCs. Some triterpenes consisting of bi- and tetracyclic skeletons have been produced in significantly high amounts by the Y609F, but no abortive cyclization product was found with Y612F.[21] However, the Ala mutants had product distribution patterns definitively different from those of the corresponding Phe mutants. Besides **2** and **3**, only a bicyclic skeleton was produced by Y609A, and two products having mono- and bicyclic skeletons were produced by Y612A. Based upon both the kinetic results and structures of the abortive cyclization products formed by the Ala mutants, we show here that the side chain of Y609 works to stabilize the C-8 carbocationic intermediate and that of Y612 to stabilize C8 and C10. Mutant Y495A afforded no abortive cyclization product, but retained half the activity of native SHC, which is in contrast to the complete loss of cyclase activity that were observed for Y495F.[21] This finding suggests that the catalytic function of the Tyr was not as crucial as that proposed by other workers.[2,21] From the mutation experiments on all conserved Phe and Tyr, we further identified residue F129 as a new active site and also found that the three residues of Y372, Y474 and Y540 reinforced the protein structure against thermal denaturation.

## Materials and Methods

*Instruments.* $^1$H- and $^{13}$C-NMR spectra were measured with a Bruker DPX 400 instrument, and MS spectra with a JEOL SX 100 mass spectrometer. GC analyses were carried out by a Shimadzu GC-8A instrument with a DB-1 capillary column (0.53 mm × 30 m).

*Regular methods.* Detailed experimental protocols have been reported in the previous papers[11,14,15] for overexpression systems with the pET vector in *E. coli* BL21(DE3), for DNA sequence analyses and for the enzyme purification methods.

*Site-directed mutagenesis.* All site-directed mutagenesis experiments were performed as described in the previous papers.[11,14,15] The following primers were used:

Y67A, 5′-pd[CTCGTGCAACAG***GGCC***CGCCGGATCTTC]-3′ (+*Kpn*I)

Y95A, 5′-pd[CCATCGAGGCG***GCC***GTCGCGCGCTCAAG]-3′ (−*Spl*I)

F129A, 5′-pd[GTCGCGCGTG***GCC***ACGCGTATGTGGCTGG]-3′ (+*Mlu*I)

Y372A, 5′-pd[GACAACGTGTAC***GCC***CCGGACGTCGACGACACGGCC]-3′ (+*Sal*I)

Y474A, 5′-pd[CCCGCTTGAG***AGC***TTCCACCGCTCGCCGGATGACC]-3′ (−*Bss*HII)

Y495A, 5′-pd[CCACCGCGCC**GGTACC*GGC***GAGGTAATTGAC]-3′ (+*Kpn*I)

Y540A, 5′-pd[CTAGAGGATCCTC***GGCA***GATCTGCAGTCCTCGCC]-3′ (+*Bgl*II)

Y606A, 5′-pd[GGTGTAGCCGAG***GGC***GAAATCCCCGGGGAAGCCCG]-3′ (+*Sma*I)

Y609A, 5′-pd[GGCGGTACATGGT***GGC***GCCGAGGTAG]-3′ (+*Bbe*I)

Y612A, 5′-pd[GGAAACACGTGGCG***GGC***CATGGTGTAGC]-3′ (+*Nco*I)

Y624A, 5′-pd[CGATGGCTTGCTT***GGC***GCGACCGAGCGCGAGC]-3′ (−*Eco*52I)

The bold letters designate the altered bases, and the target mutations are shown by the italic letters. The underlined letters show the silent mutations for easy screening of the desired mutants by a restriction fragment analysis. The created or deleted restriction sites are shown in parentheses. To ascertain that the desired mutation had been carried out, the entire region of all the inserted DNAs was sequenced.

*Thermal stability and kinetic analysis.* All the mutated SHCs were homogeneously purified according to the protocol described in the previous paper.[11,14,15] A mixed solution, which was composed of 0.5 mM squalene, 0.2% Triton X-100 and 5 $\mu$g of the homogeneously purified enzyme in a sodium citrate buffer (60 mM, pH 6.0), was prepared in a final volume of 5 ml for the enzyme reactions. Incubation was done for 60 min at different temperatures (30, 35, 40, 45, 50, 55, 60, 65, or 70°C) to examine the thermal stability of the cyclases. To determine the kinetic parameters, the incubation was conducted for 60 min at 45°C. To terminate the reaction, 15% methanolic KOH (6 ml) was added. The lipophilic products (**2** and **3**) and starting material **1**, which remained unchanged, were extracted four times with hexane (5 ml) from the reaction mixtures, and the amount of **2** thus produced was evaluated by a GC analysis with a DB-1 capillary column (30 m in length). Kinetic parameters $K_m$ and $k_{cat}$ were determined according to

the Lineweaver-Burk equation.

*Isolation and identification of 11 and 12.* The *E. coli* transformant, in which mutated Y612A SHC was expressed, was cultured at 30°C for 20 h in a Luria-Bertani medium (4 L) containing 50 mg/l of ampicillin. The cells were collected by centrifugation and washed twice with a Tris-HCl buffer (pH 8.0, 50 mM). To the collected pellets, 200 ml of a Tris buffer supplemented with 1% Triton X-100 (w/v) was added. The bacterial cells were subjected to ultrasonication at 4°C and then centrifuged to remove the cell debris to prepare a cell-free homogenate. The pH value of the supernatant was adjusted to 6.0 by adding 0.5 M citric acid. Squalene **1** (300 mg) was incubated with the homogenate at 60°C for 16 h, and the reaction mixture was lyophilised. The products were extracted three times with hexane (200 ml) from the incubation mixture, and remaining **1** was detected in a small amount by GC and TLC. The retention times of **1**, **2**, **3**, **11** and **12** by GC (30 m DB1 capillary column, 290°C injection temperature, 270°C column temperature and 1.0 kg/cm$^2$ flow rate of carrier $N_2$) were as follows: 9.4 min, 26.4 min, 36.4 min, 9.3 min, and 12.7 min, respectively. The $R_f$ values for **1**, **2**, **3**, **11** and **12** by TLC ($SiO_2$, 100% *n*-hexane) were as follows: 0.46, 0.72, 0, 0.51 and 0.55, respectively. Column chromatography over $SiO_2$ afforded **2** (265 mg), **11** (1.1 mg) and **12** (3.7 mg) by eluting with hexane, and **3** (14 mg) by eluting with a mixed solvent of hexane and EtOAc (100:2).

Compounds **11** and **12** have been previously isolated[15,16] and unequivocally identified by EIMS and detailed NMR analyses (COSY 45, HOHAHA, NOESY, DEPT, HMQC and HMBC spectra). **11** was determined to be 3-deoxyachilleol from the spectroscopic data,[15] $[\alpha]_D^{25}$ +8.02 (*c* 2.95, $CHCl_3$). Selected NMR data (in $C_6D_6$) for the bicyclic ring of **12** as $\delta_H$ (ppm): H-1 (1.07, m; 1.97, m), H-2 (1.52, m; 1.62, m), H-3 (1.28, m; 1.54, m), H-5 (1.35, m), H-6 (2.00, m; 2.08, m), H-7 (5.57, br s), H-9 (1.80), H-11 (1.45, m; 1.68, m), H-12 (2.18, m; 2.38, m), Me-23 (1.00, 3H, s), Me-24 (0.98, 3H, s), Me-25 (0.95, 3H, s), Me-26 (1.91, 3H, s); and of other protons of the isoprenoid side chain: ~5.50 (2H, br s, olefinic protons), 5.37 (1H, t-like, olefinic proton), 2.2–2.5 (8H, m, 4×C$H_2$), 1.69 (3H, s), 1.74 (3H, s), 1.77 (3H, s) and 1.80 (3H, s). $\delta_C$ (ppm) around the bicyclic skeleton: C-1 (39.5), C-2 (19.2), C-3 (42.6), C-4 (33.1), C-5 (50.4), C-6 (24.2), C-7 (122.5), C-8 (135.4), C-9 (54.5), C-10 (37.0), C-11 (27.7), C-12 (30.7), C-23 (22.1), C-24 (33.3), C-25 (13.7), C-26 (22.4), and of other carbons of the side chain: 135.0 (s), 134.9 (s), 131.1 (s), 125.4 (d), 124.9 (d), 124.8 (d), 40.2 (t), 40.2 (t), 27.2 (t), 27.1 (t), 25.8 (q), 17.7 (q), 16.2 (q), 16.1 (q). The relative stereochemistry was confirmed by NOE cross peaks between H-5, Me-24 and H-9. The double bond position was confirmed by the HMBC cross peaks from Me-26 to C-7, C-8 and C-9. EIMS fragments *m/z* (%): 410 (10) [$M^+$], 395 (3) [$M^+$-$CH_3$], 341 (3) [allylic cleavage between C-19 and C-20], 273 (3), 205 (11), 204 (18), 191 (32) [allylic cleavage between C-9 and C-11], 137 (15), 69 (100). $[\alpha]_D^{25}$ +8.9 (*c* 0.28, $CHCl_3$), *cf.* +8.7 (*c* 0.9, $CHCl_3$) in ref. 22. The cell-free homogenate of the Y609A SHC from a 50-ml culture was incubated with **1** (1 mg) at 60°C for 16 h. Four metabolites were detected by GC and TLC. These were identified as **1**, **2**, **3** and **12** by comparing the retention times from GC and the fragment patterns from GC-MS with those for Y612A.

## Results

*Characterization of all the conserved residues of Phe and Tyr*

To identify the functions of the Phe and Tyr residues conserved in the known SHCs, *in vitro* mutagenesis experiments were carried out. The functions of 11 residues of Y67, Y95, F129, Y372, Y474, Y495, Y540, Y606, Y609, Y612 and Y624 have yet to be determined (Fig. 1). The residues of Y95, Y624, F129, Y495 and Y612 were located inside either internal or external $\alpha$-helices of QW motifs. The two residues of Y606 and Y609 were composed of a $\beta$-strand structure. The other aromatic residues were situated in a loop structure connecting each $\alpha$-barrel. These aromatic residues were mutated into Ala to diminish the aromatic function. Homogeneously purified enzymes were used to assay the enzyme activity. Figures 2(a) and 2(b) show the relationship between the incubation temperature and cyclase activity for the native and mutated SHCs. The results are classified into the following three categories: (1) Y67A, Y95A, Y606A and Y624A had the same activities and optimal temperature (60°C) as those of the wild-type SHC. (2) The three mutants, Y372A, Y474A and Y540A, had nearly equivalent activities to those of the wild-type at low temperatures, but lower specific activities at high temperatures, the optimal temperatures being determined to be 55°C, 52°C and 55°C, respectively. (3) The four mutants, F129A, Y495A, Y609A and Y612A, had lower activity at the overall incubation temperatures examined, but the optimal temperatures remained unchanged.

Each incubation was carried out at pH 6.0 and 45°C for 60 min to determine the kinetic values of $k_{cat}$ and $K_m$, which were estimated from Lineweaver-Burk plots. The results are summarized in Table 1. Under these incubation conditions, no thermal denaturation was observed for any of the mutants. The 7 mutants of Y67A, Y95A, Y372A, Y474A, Y540A, Y606A and Y624, which fall into category 1 or 2, had the same kinetic values for $K_m$s and $k_{cat}$s as those of the wild-type. Thus, the 7 Tyr residues were not active sites.

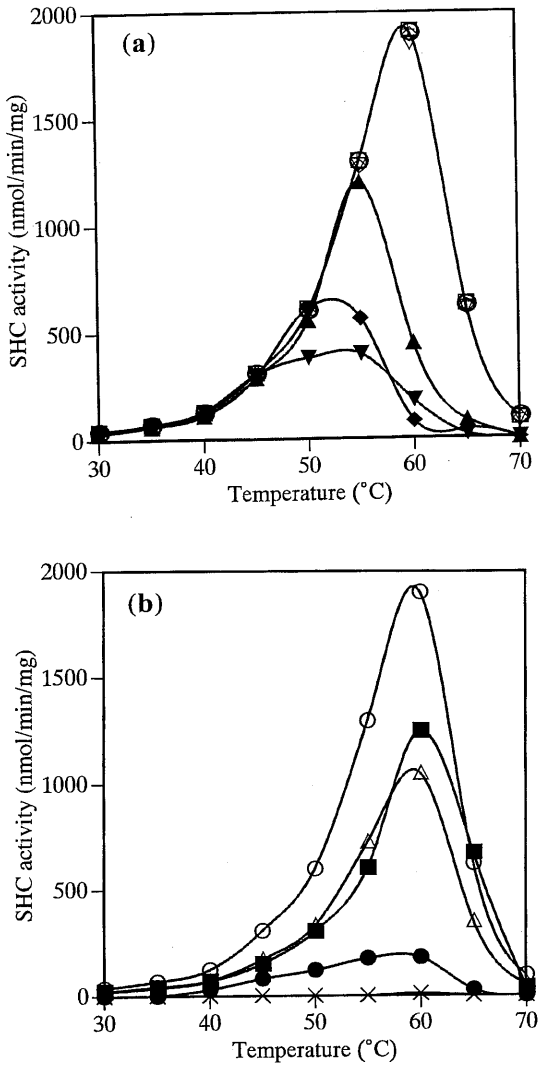


**Fig. 2.** Effect of Incubation Temperature on the Enzyme Activities of the Wild-type and Mutated SHCs targeted for All the Conserved Phe and Tyr Residues.

The specific activities are represented by the estimated amount of **2** produced.

Figure 2(a) shows the enzymes which are not responsible for the catalytic function: ○, native SHC; ▽, Y67A; +, Y95A; ▼, Y372A; ◆, Y474A; ▲, Y540A; ◇, Y606A; □, Y624A.

Figure 2(b) represents the active sites: ○, the native SHC; ●, F129A; △, Y495A; ×, Y609A; ■, Y612A.

Residues Y67 and Y474 were located in QW 5c and 3, respectively, which share two kinds of secondary structure, *i.e.* α-helix and a stacking structure of Q with W. This finding further supports the previous conclusion that none of QW motifs was an active site.[14] We presumed that residues Y372 and Y606 had an influence on the cyclization reaction, because these two residues were situated in proximity to the active sites of D374 and F605[15,17] in the primary structure (Fig. 1). However, both Y372 and Y606 were found not to be catalytic sites (Table 1). The X-ray analysis revealed that the two adjacent residues of F605 and Y606 constitute a β-strand structure,[12] indicating that the aromatic ring of Y606 was oriented in a direction opposed to that of F605; thus, Y606 could not interact with the substrate. On the other hand, the lower activities of the mutated SHCs of Y372A, Y474A and Y540A (Fig. 2(a)) would have been due to gradual degradation of the protein structure, because high energy was released during the polycyclization reaction.[12] Thus, the three residues of Y372, Y474 and Y540 possibly worked to reinforce the enzyme structure. We could not previously assign any function for QW motif 3 by mutating Trp485 into aliphatic Val,[14] but it can now be inferred that QW 3 including Y474 also works to stabilize protein structure against thermal denaturation, as was found with QW motifs 4, 5a and 5b.

The cyclase activities of the mutants of F129A, Y495A, Y609A and Y612A (category 3) were significantly lower (Table 1), indicating that the 4 residues were active sites. The mutated SHCs of F129A, Y495A and Y612A had smaller $k_{cat}$ values, 26%, 55% and 47% of the wild-type, respectively, whereas the $K_m$ values were nearly the same as those of the wild-type (Table 1). These facts suggest that the three aromatic side chains of the wild-type SHC worked to accelerate the cyclization cascade. The kinetic data for mutant Y609A could not be measured due to the nearly complete loss of cyclase activity in the overall range of temperatures examined. We have previously reported functional analyses of the three conserved Phe residues other than the aromatic residues described here. F365A SHC had also lost its cyclase activity[16] (Table 1), as was found with the Y609A mutant. The crucial function of F129 for catalytic acceleration has not been reported before.

*Product distributions of F129A, Y495A, Y609A and Y612A*

We have reported that mutated SHCs, targeted for W169 and W489, produced a partially cyclized compound having a tetracyclic skeleton (17-*epi*-dammarene).[4] Site-directed mutations for the different active sites have afforded differently cyclized products besides **2** and **3**. This product distribution was dependent on the mutants employed; monocyclic for D377C and D377N,[15] bicyclic for F365A,[16] bi- and tricyclic for Y420A,[20] tri- and tetracyclic for F601A,[5] tri-, tetra- and pentacyclic for F605A,[17] and tri-, tetra- and pentacyclic for I261A.[6] These partially cyclized products were each generated from carbocation intermediates **4**–**10** (Scheme 1). In contrast, mutants have also been found which showed a product distribution similar to that of the wild-type without any abortive cyclization product having been formed, as exemplified by D374N, D376N, W312L, H451F, D313N, and D447N.[14,15] These residues are responsible for initiating the cyclization cascade (Scheme 1). Thus, an analysis of the product distribution is very useful for identifying the active sites and for giving insight into the functions of the active

**Table 1.** Kinetic Data and Optimal Temperatures for the Wild-type and Mutant SHCs Targeted for All the Conserved Phe and Tyr Residues in SHCs

The kinetic values for $K_m$ and $k_{cat}$ were determined from Lineweaver-Burk plots. The enzyme activities were assayed for the purified SHCs (5 $\mu$g) by estimating the amount of **2** produced by incubating at 45°C for 60 min, under the condition of the purified proteins not being denatured.

| SHC | Category* or Reference | $K_m$ ($\mu$M) | $k_{cat}$ (min$^{-1}$) | $k_{cat}/K_m$ | Relative activity (%) | Optimal temperature for 60 min (°C) |
|---|---|---|---|---|---|---|
| Wild-type | | $1.62\times10$ | 51.8 | 3.19 | 100.0 | 60 |
| Y67A | (1) | $1.67\times10$ | 51.2 | 3.07 | 96.2 | 60 |
| Y95A | (1) | $1.67\times10$ | 50.2 | 3.01 | 94.4 | 60 |
| Y606A | (1) | $1.69\times10$ | 50.7 | 3.00 | 94.0 | 60 |
| Y624A | (1) | $1.69\times10$ | 51.0 | 3.02 | 94.7 | 60 |
| Y372A | (2) | $1.63\times10$ | 53.1 | 3.26 | 102.2 | 55 |
| Y474A | (2) | $1.60\times10$ | 51.2 | 3.20 | 100.3 | 52 |
| Y540A | (2) | $1.61\times10$ | 49.8 | 3.09 | 96.9 | 55 |
| F129A | (3) | $1.85\times10$ | 13.7 | $7.41\times10^{-1}$ | 23.2 | 60 |
| Y495A | (3) | $1.72\times10$ | 28.7 | 1.67 | 52.4 | 60 |
| Y609A** | (3) | — | — | — | 0 | 60 |
| Y612A | (3) | $1.33\times10$ | 24.4 | 1.83 | 57.4 | 60 |
| D377N** | Ref. 15 | — | — | — | 0 | 60 |
| F365A** | Ref. 16 | — | — | — | 0 | 55 |

* The categories were classified according to the relationship between the incubation temperature and specific activities (Fig. 2).
** The kinetic values could not be determined due to markedly decreased activity.

**Table 2.** Product Ratios (%) of the Wild-type and Mutant SHCs targeted for the Active Components

One mg of **1** was incubated with the cell-free lysate, which had been prepared from 50-ml cell culture, under the condition of pH 6.0, 60°C and 16 h. The cell-free homogenate included 0.5 mg of the pure SHCs, which was 100-fold more than that employed for the kinetic studies (5 $\mu$g). Each product ratio was estimated by a GC analysis.

| SHC | Hopene **2** | Hopanol **3** | 3-Deoxyachilleol **11** | $\gamma$-Polypodatetraene **12** |
|---|---|---|---|---|
| Wild-type | 84.1 | 15.9 | — | — |
| F129A | 84.5 | 15.5 | — | — |
| Y495A | 84.8 | 15.2 | — | — |
| Y609A | 41.9 | 8.3 | — | 49.8 |
| Y612A | 76.9 | 15.3 | 2.2 | 5.6 |

sites.

One mg of substrate **1** was incubated at pH 6.0 and 60°C for 16 h by using a large amount of the cell-free lysate corresponding to 0.5 mg of the pure SHCs. The hexane extract from the reaction mixture was loaded into a short $SiO_2$ column and eluted with a mixture of hexane/EtOAc (100:20) to remove Triton X-100. The product distributions were analyzed by GC chromatography (Table 2). The mutated SHCs of F129A and Y495A afforded **2** and **3** without the accumulation of any abortive cyclization product. In addition, the amounts of **2** and **3** produced were almost the same as that of the wild-type (Table 2). On the other hand, Y609A produced **12**, while Y612A afforded **11** and **12**, together with **2** and **3** (Table 2 and Fig. 3). **11** was also isolated from mutants D377C and D377N.[15] The structure of **12** has been determined to be $\gamma$-polypodatetraene[22] from a detailed NMR analysis, which was also produced by mutants F365A[16] and Y420A.[20] **11** and **12** could be produced by a deprotonation reaction from intermediates **4** and **5**, respectively (Scheme 1 and Fig. 3). Proton elimination occurred from Me-27 from **4** to give **11**, while deprotonation from H-7 from **5** afforded **12**. Functional analyses of Y495, Y609 and Y612 have very recently been reported that were inferred by mutating into a similar aromatic Phe.[21] The product distributions of mutated Y609A and Y612A markedly differed from those of Y609F and Y612F. Mutant Y612A produced mono- and bicyclic skeletons **11** and **12**, whereas the Phe mutant accumulated no partially cyclized product. Mutant Y609A accumulated bicyclic **12** alone. In contrast, the Phe mutant accumulated 6 new triterpenes in significantly high amounts, consisting of one bi- **13** ($\alpha$-polypodatetraene)[22] and five tetracyclic skeletons arising from **8** (bi-:tetracyclic:**2** = 4.5%:46.2%:49.3%).[21]

The product distribution of the other mutants, classified into categories 1 and 2, were the same as that of the wild-type, no abortive cyclization product being accumulated.

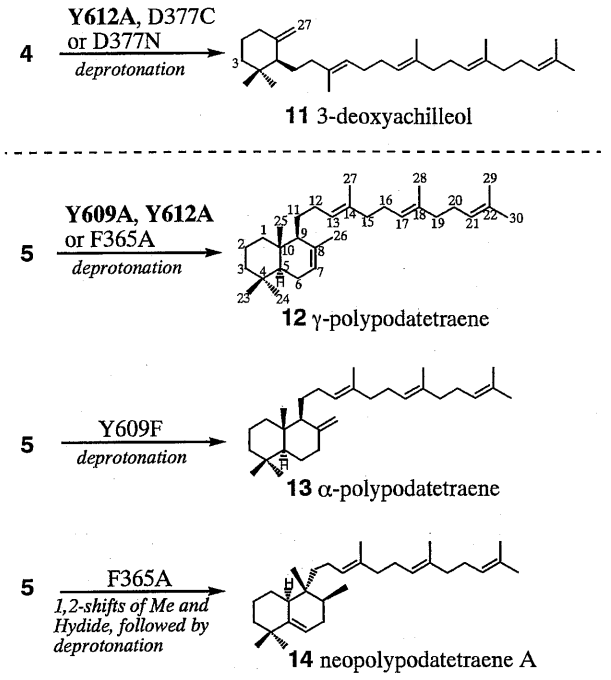


**Fig. 3.** Structures of the Abortive Cyclization Products Accumulated by the Mutated SHCs.

## Discussion

We have demonstrated in the previous paper[15] that residues D374 and D376 serves the acidic proton to initiate the cyclization cascade, and that D377 stabilized the C10 cation of **4**. It was also suggested that H451 acted as a proton acceptor to enhance the acidity of D374 and/or D376 and that the two acidic residues of D313 and D447 may facilitate initiation of the cyclization reaction. According to an X-ray analysis, Wendt *et al.* have proposed that acidic D376 would serve the proton donor to initiate polycyclization, and that the anion of D374, through hydrogen-bonding with D377, may accommodate a positive charge on the D376:H451 pair (Fig. 4).[12,13] Our point mutation results were in good agreement with the proposal from the three-dimensional structure, as most recently reviewed by Wendt *et al.*[2] The X-ray structure also revealed that the hydroxyl group of Y495 was connected *via* a water bridge to protonating D376, whereby protonation to the folded squalene supplied by D376 may be promoted due to the enhanced acidity of D376 (Fig. 4).[13] No partial cyclization product was accumulated by mutant Y495A (Table 2), suggesting that Y495 was oriented near the initiation site. Füll and Poralla have reported that Y495F had no enzyme activity and thus inferred that the phenolic hydroxyl group was crucial for catalysis.[21] This may be consistent with the proposal that Y495 enhances the acidity of D376, resulting in facilitation of the start of cyclization by protonation. However, the Y495A mutant still retained 52% of the activity of the wild-type (Table 1), despite the hydro-

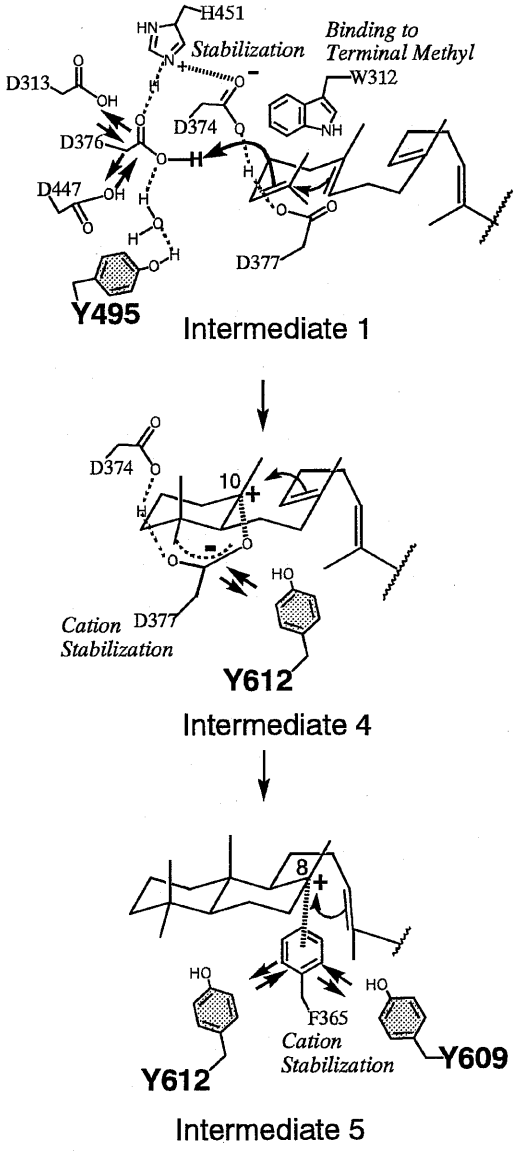


**Fig. 4.** Proposed Model of the Catalytic Mechanism for SHC from the Initiation Reaction Step Triggered by Protonation to Five-membered C-ring Closure.

This model is based on the results of site-directed mutagenesis experiments[14-16] and the three-dimensional crystal structure.[12,13]

Top: The cyclization cascade is initiated by the acidic proton of D376, the acidity of which is enhanced by the combination of D374, H451 and Y495, as revealed by the 2.0 Å resolution X-ray structure.[13] The hydroxyl group of Y495 is hydrogen-bonded with D376 *via* a water molecule. The acidic residues of D313 and D447 are also responsible for the initiating cyclization,[15] although the molecular mechanism for enhancing the acidity of D376, which is designated by the symbol ⇆, remains unknown. Trp312 is likely to work to arrest the terminal isopropylidene methyl group(s), based upon the kinetic results.[14] This mechanism is conflict with the proposal by other workers that W312 stabilizes the C4 carbocation *via* a cation-π interaction.

Center and Bottom (intermediates **4** and **5**): The C-8 and C-10 cations of **4** and **5** are respectively stabilized by the carboxylate anion of D377 and by π-electrons of F365 *via* cation-π interaction.[15,16] Y612 and Y609 may work to place D377 and F365 at the correct positions in the enzyme cavity and to enrich the negative charge of D377 and the π-electrons of F365, so that D377 and F365 can effectively stabilize their carbocationic intermediates **4** and **5**. The symbol ⇆ shows the presence of such interaction(s) among D377, F365, Y609 and Y612.

gen bond being missing like the Phe mutant. This finding is inconsistent with the inference drawn by other workers.[13,21] The reason why the Ala mutant had higher catalytic activity than the Phe mutant is not clear. When hydrogen-bonding *via* a water-bridge is not possible due to the absence of a phenolic hydroxyl group, the steric bulk size may in turn have a significant influence on the cyclization cascade. The larger steric bulk size of Phe, compared to Ala, may have interfered with the most favorable binding to the product-like conformation of **1** that was formed prior to the start of cyclization, but further knowledge is required to confirm this. The kinetic data for the W312 mutant have suggested that the major function of W312 is binding to **1**, and not cation stabilization *via* the cation-$\pi$ interaction (Fig. 4); the $K_m$ value for W312F was markedly higher, but the $k_{cat}$ value remained unchanged.[14] This is also inconsistent with the proposal by Wendt *et al.* that W312 works to stabilize the C4-carbocation intermediate (hopene numbering). In the previous paper,[23] we have demonstrated that two methyl groups were indispensable for initiating the polycyclization cascade. Trp312 is likely to act for binding to the terminal methyl groups of **1**. We suggest that CH-$\pi$ interaction[24] may be involved between the terminal methyl(s) of **1** and the aromatic $\pi$-electrons of Trp, although this concept is not widely accepted in respect of triterpene cyclases. CH-$\pi$ interaction is enhanced with increasing electron density.[24]

Bicyclic **12** was accumulated by mutant Y609A along with **2** (Table 2), suggesting that Y609 stabilized the C-8 carbocation of bicyclic **5**, leading to subsequent C-ring formation (Scheme 1 and Fig. 4). The production of two bicyclic compounds, **12** and **14**, *via* **5** was also observed for mutant F365A.[16] However, the yields of the bicyclic compounds were different. The higher yield of 96% for **12** and **14** by F365A,[16] than of ca. 50% by Y609A (Table 2) suggests that the carbocation stabilization of **5** may have been achieved mainly by the $\pi$-electrons of F365 with the aid of those of Y609. We have not given a name to **14** in the previous literature,[16] although it is an "unnatural natural product" which has not previously been found in nature. We propose here the name neopolypodatetraene A for **14**. In contrast to mutant Y609A prepared by us, one bicyclic and five tetracyclic products were accumulated by mutant Y609F.[21] A high production of tetracyclic triterpenes (46.2%), compared to bicyclic **13** (4.5%), has made it difficult to propose the exact location and function of Y609. However, the production of only bicyclic **12** by the Ala mutant strongly indicates that the location of Y609 was very close to F365 (Fig. 4). The phenolic hydroxyl group of Y609 may work to place F365 at the correct position so that the most favorable cation-$\pi$ interaction can be acquired between F365 and the C-8 cation of **5**, otherwise the $\pi$-electron density of F365 may be further enriched by neighboring Y609. When the hydroxyl group is missing, the cyclization cascade proceeds toward tetracyclic intermediate **8**, suggesting that a perturbation around C-8 and/or lowering the $\pi$-electron density of F365 is not significant by the mutation of Y into F. However, mutant Y609A had no $\pi$-electrons and underwent marked perturbation due to the decreased bulk size around the active site, thus ending polycyclization at the bicyclic reaction stage.

The function of Y612 has not clearly been referred to by the X-ray analysis.[12,13] Füll and Poralla have assumed that Y612 was involved in the initiation reaction, because the product distribution pattern was the same as that of native SHC and no partially cyclized product was accumulated by mutating Tyr into Phe.[21] However, the Ala mutant produced monocyclic **11** (2%) and bicyclic **12** (6%) (Fig. 3 and Table 2), suggesting that Y612 stabilized cation intermediates **4** and **5** (Scheme 1, Fig. 4), which is in contrast to the suggestion proposed by Füll and Poralla.[21] The yields of **11** and **12** were low, compared to those of D377 and F365: 90% of monocyclic **11** for D377C, and 96% of bicyclic **12** and **14** for F365A.[15,16] Y612 may intensify each function of both D377[15] and F365,[16] possibly by placing D377 and F365 at positions favorable enough to stabilize cations **4** and **5** (Fig. 4). The loss of $\pi$-electrons and the phenolic hydroxy group in mutant Y612A could not amplify the negative charge of D377 and the $\pi$-electron density of F365, thus resulting in a slower reaction rate (Table 1). The $K_m$ value remained unchanged (Table 1), suggesting that perturbation around the active site was little affected by the Y→A replacement.

The crucial role of F129 in the catalysis has not been suggested before. F129A did not accumulate any new products (Table 2), suggesting that F129 would not be aligned near any discrete carbocations that have been generated during the polycyclization reaction (Scheme 1). However, it is unlikely that F129 works to initiate cyclization. An X-ray analysis has shown that conserved F129 was situated near the substrate entrance or product exit channel.[12,13] With regard to the amino acid residues located near the substrate access, no point mutation experiments have been reported, except for E45.[15,25] It has been demonstrated by mutating Glu45 into Ala and Asp that the nucleophilicity of the E45 carboxylate anion was important for the catalysis.[25] This agrees with the X-ray suggestion that a hydrogen-bonded network of Q262:E45:Q93:R127 involving a water molecule may stabilize or quench the C-22 carbocation of **10**.[12,13,25] To address the function of F129, more detailed mutation experiments are required, which should be targeted at other amino acid residues located near the substrate entrance, in addition to replacement experiments by other differently catego-

rized amino acids with different electronic and/or bulk size environments.

The mutagenesis experiments described here on highly conserved Phe and Tyr into Ala give greater insight into the functions and the location sites in the cyclase cavity. We could further identify QW motif 3 as a new stabilization site against thermal denaturation, in addition to previously assigned three QW motifs 4, 5a and 5b.[14] We have previously suggested that QW motifs may play important roles in maintaining enzyme structures against severe circumstances such as high temperature (*A. acidocaldarius*) and a high concentration of ethanol (*Z. mobilis*).[14]

The product distribution difference between the Ala and Phe mutants is dependent on the presence or absence of aromatic $\pi$-electrons. Since we have completed the mutation experiments on all the conserved Trp residues and examined the kinetic data in detail,[14] the catalytic role of the aromatic Phe, Tyr and Trp residues in squalene cyclization may be summarized. It has been proposed that aromatic Phe, Tyr or Trp work to stabilize the transient carbocation intermediate *via* cation-$\pi$ interaction.[26,27] Recent mutation experiments on F365[16] and F605[17] carried out by us have validated the cation-$\pi$ interaction concept. As another function of aromatic residues, the fixation and/or recognition to substrate **1** may be also proposed, as has been found with W169 and W312.[4,14] As the driving force, CH-$\pi$ interaction may be plausible between the alkyl proton(s) and $\pi$-electrons of the Trp side chain. In this study, some aromatic residues were found to reinforce and/or further intensify the functions of residues critical to the catalysis, as exemplified by Y609 and Y612. It is likely that Y609 and Y612 work to place D377 and F365 at the most favorable positions for cyclization catalysis. The importance of F129 in the cyclization reaction, which has never been pointed out before, was disclosed through the point mutation experiments targeted at all the conserved Phe and Tyr residues. The functional analyses of some amino acid residues, including F129, which are located near the substrate entrance channel, will be reported in due course.

## Acknowledgment

This work was supported by grant-aid to T.H. (No. 11660104) and by grant-aid for a JSPS Fellow to T.S. from the Ministry of Education, Science and Culture of Japan. We are also indebted to the financial support by the Fujisawa Foundation which was given to T.H.

## References

1) Abe, I., Rohmer, M., and Prestwich, G. D., Enzymatic cyclization of squalene and oxidosqualene to sterols and triterpenes. *Chem. Rev.*, **93**, 2189–2206 (1993).
2) Wendt, K. U., Schulz, G. E., Corey, E. J., and Liu, D. R., Enzyme mechanisms for polycyclic triterpene formation. *Angew. Chem. Int. Ed.*, **39**, 2812–2833 (2000).
3) Hoshino, T., Insight into the active sites of squalene cyclase and the cyclization mechanism (in Japanese). *Bioscience & Industry*, **59**, 167–170 (2001).
4) Sato, T., Abe, T., and Hoshino, T., On the cyclization mechanism of squalene: a ring expansion process of the five-membered D-ring intermediate. *J. Chem. Soc. Chem. Commun.*, 2617–2618 (1998).
5) Hoshino, T., Kouda, M., Abe, T., and Ohashi, S., New cyclization mechanism of squalene: a ring expansion step of the five-membered C-ring intermediate in hopene biosynthesis. *Biosci. Biotechnol. Biochem.*, **63**, 2038–2041 (1999).
6) Hoshino, T., Abe, T., and Kouda, M., Unnatural natural triterpenes produced by altering isoleucine into alanine at position 261 in hopene synthase and the importance of having the appropriate bulk size at this position for directing the stereochemical destiny during the polycyclization cascade. *J. Chem. Soc. Chem. Commun.*, 441–442 (2000).
7) Pale-Grosdemange, C., Feil, C., Rohmer, M., and Poralla, K., Occurrence of cationic intermediate and deficient control during enzymatic cyclization of squalene to hopanoids. *Angew. Chem. Int. Ed.*, **37**, 2237–2240 (1998).
8) Kannenberg, E. L. and Poralla, K., Hopanoid biosynthesis and function in bacteria. *Naturwissenschaften.*, **86**, 168–176 (1999).
9) Shibuya, M., Zhang, H., Endo, A., Shishikura, K., Kushiro, T., and Ebizuka, Y., Two branches of the lupeol synthase gene in the molecular evolution of plant oxidosqualene cyclases. *Eur. J. Biochem.*, **266**, 302–307 (1999).
10) Godzina, S., Lovato, M. A., Meyer, M. M., Foster, K. A., Wilson, W. K., Gu, W., de Hostos, E. L., and Matsuda, S. P. T., Cloning and characterization of the *Dictyostelium discoideum* cycloartenol synthase cDNA. *Lipids*, **35**, 249–255 (2000).
11) Sato, T., Kanai, Y., and Hoshino, T., Overexpression of squalene-hopene cyclase by the pET vector in *Escherichia coli* and first identification of tryptophan and aspartic acid residues inside the QW motif as active sites. *Biosci. Biotechnol. Biochem.*, **62**, 407–411 (1998).
12) Wendt, K. U., Poralla, K., and Schulz, G. E., Structure and function of a squalene cyclase. *Science*, **277**, 1811–1815 (1997).
13) Wendt, K. U., Lenhart, A., and Schulz, G. E., The structure of the membrane protein squalene-hopene cyclase at 2.0 Å resolution. *J. Mol. Biol.*, **286**, 175–187 (1999).
14) Sato, T. and Hoshino, T., Kinetic studies on the function of all the conserved tryptophans involved inside and outside the QW motifs of squalene-hopene cyclase: stabilizing effect of the protein structure against thermal denaturation. *Biosci. Biotechnol. Biochem.*, **63**, 1171–1180 (1999).
15) Sato, T. and Hoshino, T., Functional analysis of the DXDDTA motif in squalene-hopene cyclase by site-

directed mutagenesis experiments: initiation site of the polycyclization reaction and stabilization site of the carbocation intermediate of the initially cyclized A-ring. *Biosci. Biotechnol. Biochem.*, **63**, 2189–2198 (1999).

16) Hoshino, T. and Sato, T., Functional analysis of phenylalanine 365 in hopene synthase, a conserved amino acid in the families of squalene and oxidosqualene cyclases. *J. Chem. Soc. Chem. Commun.*, 2005–2006 (1999).

17) Hoshino, T., Kouda, M., Abe, T., and Sato, T., Functional analysis of Phe605, a conserved aromatic amino acid in squalene-hopene cyclase. *J. Chem. Soc. Chem. Commun.*, 1485–1486 (2000).

18) Feil, C., Sussmuth, R., Jung, G., and Poralla, K., Site-directed mutagenesis of putative active-site residues in squalene-hopene cyclase. *Eur. J. Biochem.*, **242**, 51–55 (1996).

19) Merkofer, T., Pale-Grosdemange, C., Wendt, K. U., Rohmer, M., and Poralla, K., Altered product pattern of a squalene-hopene cyclase by mutagenesis of active site residues. *Tetrahedron Lett.*, **40**, 2121–2124 (1999).

20) Pale-Grosdemange, C., Merkofer, T., Rohmer, M., and Poralla, K., Production of bicyclic and tricyclic triterpenes by mutated squalene-hopene cyclase. *Tetrahedron Lett.*, **40**, 6009–6012 (1999).

21) Füll, C. and Poralla, K., Conserved Tyr residues determined function of *Alicyclobacillus acidocaldarius* squalene-hopene cyclase. *FEMS Microbiol. Lett.*, **183**, 221–224 (2000).

22) Shiojima, K., Arai, Y., Masuda, K., Kamada, T., and Ageta, H., Fern constituents: polypodatetraenes, novel bicyclic triterpenoids, isolated from *polypodiaceous* and *aspidiaceous* plants. *Tetrahedron Lett.*, **24**, 5733–2736 (1983).

23) Hoshino, T. and Kondo, T., The cyclization mechanism of squalene in hopene biosynthesis: the terminal methyl groups are critical to the correct folding of this substrate both for the formation of the five-membered E-ring and for the initiation of the polycyclization reaction. *J. Chem. Soc. Chem. Commun.*, 731–732 (1999).

24) Nishino, M. and Hirota, M., CH/$\pi$ interaction: implication in organic chemistry. *Tetrahedron*, **45**, 7201–7245 (1989).

25) Dang, T. and Prestwich, G. D., Site-directed mutagenesis of squalene-hopene cyclase: altered substrate specificity and product distribution. *Chem. Biol.*, **7**, 643–649 (2000).

26) Shi, Z., Buntel, C. J., and Griffin, J. H., Isolation and characterization of the gene encoding 2,3-oxidosqualene-lanosterol cyclase from *Saccharomyces cerevisiae*. *Proc. Natl. Acad. Sci. USA*, **91**, 7370–7374 (1994).

27) Dougherty, D. A., Cation-$\pi$ interactions in chemistry and biology: a new view of benzene, Phe, Tyr, and Trp. *Science*, **271**, 163–168 (1996).